ANTHROPOLOGY

Evolution of brain lateralization: A shared hominid pattern of endocranial asymmetry is much more variable in humans than in great apes

Simon Neubauer[1]*, Philipp Gunz[1], Nadia A. Scott[1], Jean-Jacques Hublin[1,2], Philipp Mitteroecker[3]

Brain lateralization is commonly interpreted as crucial for human brain function and cognition. However, as comparative studies among primates are rare, it is not known which aspects of lateralization are really uniquely human. Here, we quantify both pattern and magnitude of brain shape asymmetry based on endocranial imprints of the braincase in humans, chimpanzees, gorillas, and orangutans. Like previous studies, we found that humans were more asymmetric than chimpanzees, however so were gorillas and orangutans, highlighting the need to broaden the comparative framework for interpretation. We found that the average spatial asymmetry pattern, previously considered to be uniquely human, was shared among humans and apes. In humans, however, it was less directed, and different local asymmetries were less correlated. We, thus, found human asymmetry to be much more variable compared with that of apes. These findings likely reflect increased functional and developmental modularization of the human brain.

INTRODUCTION

Anatomical and functional brain asymmetries have been described not only in humans but also in other vertebrate and even invertebrate animals (*1*). However, humans are assumed to stand out in having a specific spatial pattern of brain asymmetry that is highly directional and underlies functional and behavioral lateralization, including hemispheric specialization for complex cognitive abilities (*2*–*6*). For example, Broca's area in the inferior frontal gyrus, an important region for speech production, is usually larger in the left hemisphere, which is also the functionally dominant side (*2*) [but see (*3*)]. Furthermore, the central sulcus (separating the primary motor cortex in the frontal lobe and the primary somatosensory cortex in the parietal lobe) is deeper and longer with increased cortical folding in the left hemisphere of right-handers (i.e., the contralateral side responsible for the right body side) (*7*–*9*). Similarly, the hand motor region within the central sulcus is more dorsally located in the left hemisphere of right-handers (*10*). These patterns of "directional asymmetry" (*11*) are shared among most individuals and considered to be under strong genetic control (*12*), although a recent study did not find significant heritability in directional asymmetry (*13*). Some individuals, however, can show the reverse of the prevalent pattern within a population; this special case of a directional pattern is called "antisymmetry" (*11*). For example, although most humans are right-handers, about 10% show reversed central sulcus asymmetries and preferentially use their left hand (*14*). Reports of population-level asymmetries, such as handedness, in nonhuman primates are controversially discussed (*1*, *15*), implying that brain lateralization is most consistent, directed, and pronounced in humans. In addition to directional asymmetry, the left and right brain hemispheres can vary without clear directionality in a population. This "fluctuating asymmetry" (*11*) is thought to result from random developmental variation and developmental instabilities (*16*) unrelated to specific brain functions and has also been interpreted as a sign of developmental plasticity (*17*).

Several evolutionary hypotheses (*18*–*20*) have linked human brain asymmetry to handedness, tool use, and language. In this context, brain lateralization for sensorimotor functions is widely assumed to provide increased neural capacity, which ultimately facilitated the evolution of higher cognitive abilities in the human lineage (*21*). Comparative studies of brain asymmetry are therefore crucial for understanding the evolution and function of the modern human brain. However, difficulties in quantifying individual variation in brain asymmetry, restricted access to nonhuman comparative samples of hominids (extant relatives of humans, i.e., great apes), and the fact that brains do not fossilize hinder these investigations.

Direct evidence of brain evolution in hominins (fossil ancestors and relatives of humans) comes from fossilized bony braincases and endocranial casts (Fig. 1A). Because of the tight interactions between the brain, connective tissues (meninges), and neurocranial bones during growth (*22*), these endocasts closely reflect the size and outer shape of the brain (*23*, *24*), including the magnitude and pattern of overall brain asymmetry (*25*–*29*). However, endocasts only reflect external brain structures and their surrounding tissues; not all gyri and sulci reliably leave endocranial impressions. While endocasts can therefore only reflect certain aspects of brain asymmetry, they also offer some advantages over the analysis of brain tissue: (i) Unlike postmortem brains, endocasts do not suffer from shrinkage, and (ii) high-resolution data of endocasts are available for large samples of numerous primate taxa, whereas brain scans (of sufficient resolution) are rare, impeding comparative studies of brain variation and asymmetry.

Traditionally, endocranial asymmetries have been discussed in terms of petalias—protrusions of the cerebral cortex into the internal table of the cranial bone—and asymmetries of Broca's cap, the endocranial area corresponding to the Broca's area in the third frontal convolution (*23*). Humans typically show a left occipital petalia combined with a right frontal petalia (Fig. 1C); i.e., their left occipital lobes are wider and extend further back, whereas their right frontal lobes are wider and sometimes project more rostrally (*23*, *26*, *28*, *29*). This pattern was also found in brain imaging studies (*2*, *4*, *5*) (Fig. 1B) and showed a strong association with right handedness, whereas the reversed asymmetry pattern was—albeit to a lesser

[1]Department of Human Evolution, Max Planck Institute for Evolutionary Anthropology, Leipzig, Germany. [2]Collège de France, 11 Place Marcelin Berthelot, 75005 Paris, France. [3]Department of Evolutionary Biology, University of Vienna, Vienna, Austria. *Corresponding author. Email: simon.neubauer@eva.mpg.de

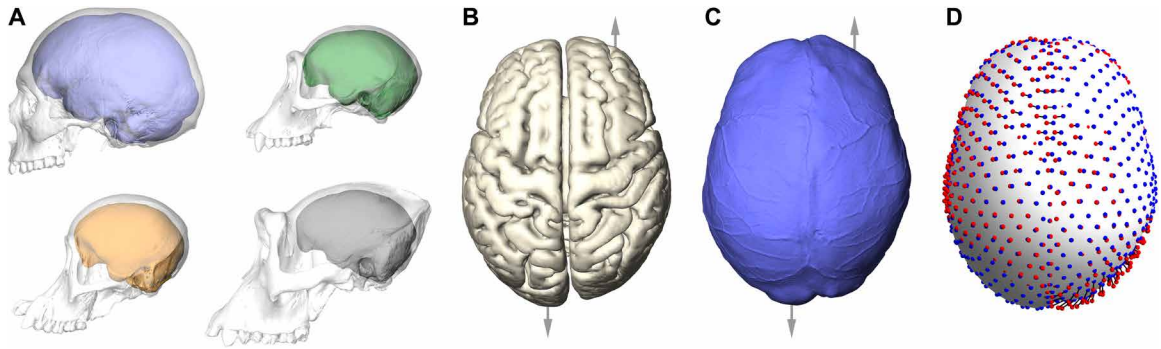

Fig. 1. Brains, endocasts, and landmarks. (**A**) Casts of the internal bony braincase (endocasts) approximate the size and outer shape of the brain in humans (blue), chimpanzees (green), gorillas (black), and orangutans (orange). (**B** and **C**) Asymmetries of the brain, such as frontal and occipital petalias (differential projections of the left and right side indicated by arrows), are observable also on the endocast. (**D**) In this study, the differences (black lines) between an endocranial landmark configuration (blue spheres) and its relabeled reflection (red spheres) were used as a measure for the magnitude and spatial pattern of shape asymmetry without the need to define a midsagittal plane or any other external reference system.

degree—related to left handedness (*23*, *29*). The brains of great apes, with a size of about a third of that of human brains (Fig. 1A), also have frontal and occipital petalias (*23*, *25*, *26*, *28*, *29*). However, a comprehensive comparison (*25*) suggested that nonhuman apes do not consistently show the combination of left occipital and right frontal petalias that is typical for humans: The anteroposterior component of this combination was found only in 39% of bonobos, 36% of chimpanzees, and 32% of gorillas. A larger portion within these three great ape taxa did not show a combination of frontal and occipital petalias on contralateral sides at all (i.e., 45, 42, and 45% of bonobos, chimpanzees, and gorillas, respectively, had a frontal petalia on the same side as an occipital petalia) (*25*). Furthermore, the degree of petalial asymmetries was found to be smaller in great apes than in humans (*26*). In other words, while some nonhuman individuals do display the typical human pattern of right frontal and left occipital petalias, great apes do not show a clear population-level directionality (*23*, *25*, *26*, *28*, *29*). Hominins seem to show the typical modern human asymmetry pattern (*23*, *26*). However, analyses of fossil hominins are complicated by the difficulties to disentangle taphonomic distortions from biological asymmetry. In addition to petalias, a leftward asymmetry of the Broca's cap was described both for modern humans and extinct hominins (*23*, *27*). A recent quantitative approach found that the third frontal convolution in human endocasts projects more laterally and anteroposteriorly on the right side so that the Broca's cap appears more globular and better defined on the left side (*27*). This study also suggested that Broca's cap asymmetry was similar in hominins and bonobos (*27*). Many previous studies relied on linear dimensions of petalias and the Broca's cap, without quantifying the actual three-dimensional shape of the brain surface or endocranium. Also, most studies focused on average asymmetry patterns and neglected individual variation in pattern and magnitude of asymmetry.

In this study, we used geometric morphometrics (*30*, *31*) and a suite of multivariate statistical tools to quantify and compare the spatial pattern and magnitude of global endocranial shape asymmetry in humans and great apes. We used 935 three-dimensional measurement points (anatomical landmarks and sliding semilandmarks) (*32*) to capture a global endocranial form in a comprehensive sample of 228 modern humans, chimpanzees, gorillas, and orangutans (see Methods and fig. S1). We did not include landmarks defined on cortical features because brain sulci and gyri are difficult to locate on endocasts and often are visible only as an approximate area, not as an exact point location. Instead, our landmark set describes overall global brain surface asymmetry including differential projections such as occipital and frontal petalias. In contrast to classic distance measurements, our approach preserves the spatial relationships between the measurements and, thus, permits the analysis and visualization of the full endocranial shape (fig. S1). Geometric morphometrics also allows for an explicit decomposition of symmetric and asymmetric shape components (*31*, *33*, *34*). To this end, each individual's landmark configuration is reflected (mirror imaged), and left landmarks that have been reflected to the right side are relabeled as right landmarks and vice versa (Fig. 1D). After superimposition, the average of a landmark configuration and its relabeled reflection is perfectly symmetric. Symmetric shape variation can, thus, be studied within the sample of "symmetrized" configurations. The difference between a configuration and its relabeled reflection, by contrast, represents the shape asymmetry of this configuration (see Methods; Fig. 1D). It can be conceived as a high-dimensional vector in shape space that contains the deviations from symmetry for all of the landmarks and semilandmarks (see Methods). The length (vector norm) of such an asymmetry vector is interpreted as the total magnitude of shape asymmetry, independent of the direction of the vector, which specifies the spatial pattern of asymmetry. Note that a perfectly symmetric object is identical to its reflection and therefore has a zero asymmetry vector. The sample of these high-dimensional asymmetry vectors serves as the basis for studying the average and variation in shape asymmetry within a population. To this end, we show how to ordinate asymmetric components of endocranial shape by a modified version of principal component analysis (PCA; see Methods). This morphometric approach does not require the specification of a global anatomical midplane to quantify asymmetry nor is an orientation or mapping to any external reference system required. Instead, asymmetry measures are based on the Procrustes metric as has been successfully used in other asymmetry studies (*13*, *17*, *33*). Note that the midsagittal (unpaired) landmarks included here were not used to define the global plane of symmetry but were themselves subjected to the asymmetry analyses (see Methods; Fig. 1D). Furthermore, because of the explicit quantification of endocranial shape—the geometric properties independent of location, scale, and orientation—we could study the degree to which shape asymmetry is attributable to endocranial size, both within and

between species. Using geometric morphometrics and multivariate statistics, we attempted to overcome the typological view of brain asymmetry, which enumerates isolated features that are, on average, larger on one side than on the other side, without reference to individual variation in pattern and magnitude of shape asymmetry. Instead, we sought after individual and shared aspects of pattern and magnitude of endocranial global shape asymmetry within humans, chimpanzees, gorillas, and orangutans. In particular, we aimed to reexamine previous findings that great apes are less asymmetric in magnitude and less consistent (less directed) in the pattern of shape asymmetry than humans.

RESULTS

Symmetric shape variation among taxa

In a PCA of the symmetric aspects of endocranial shape (Fig. 2A), the first principal component (PC 1, accounting for 59.4% of total shape variance) clearly differentiated between nonhuman apes and humans. It represented the difference between low, elongated endocasts with extended cranial bases and high, globular endocasts with flexed cranial bases. PC 2 (12.8% of total variance) corresponded to the overall length-to-width ratio: Individuals with negative scores had a narrow and long endocast, while individuals with positive scores had a short and wide endocast. This second PC represented the major axis of variation in humans and also distinguished between gorillas, chimpanzees, and orangutans. Hence, our endocranial landmark set successfully captured previously described differences in endocranial shape among these species (*35*–*37*). This symmetric shape variation accounted for 95.6% of total shape variation among the analyzed taxa, only 4.4% were attributable to individual differences in endocranial asymmetry.

Asymmetric shape variation among taxa

Because the asymmetry vectors are deviations from perfect symmetry (their natural origin), we used a modified version of PCA that maximizes the sum of squares around the symmetric origin rather than around the sample mean (see Methods). The individual PC scores then represent deviations from symmetry and are best displayed as arrows from the origin of the coordinate system (see fig. S2). Note that these arrows represent the asymmetry scores of the individuals, not the loadings of the variables, as common in PCA biplots. The length of an arrow approximates the overall magnitude of asymmetry, whereas the direction represents the spatial pattern of asymmetry. For instance, two arrows in opposite directions indicate opposite spatial patterns of asymmetry. Two arrows in a similar direction but of different length indicate specimens with a similar spatial pattern of asymmetry but different magnitudes (fig. S2D). The directionality of asymmetry within a sample can be inferred from the shared direction of the asymmetry vectors along the PCs (fig. S2, E to G).

In this PCA of endocranial shape asymmetry (Fig. 2, B and C), human and ape individuals largely overlapped, suggesting similar distributions of both pattern and magnitude of endocranial asymmetry. The first PC represented a directional asymmetry pattern that was shared among the four taxa: 76% of arrows were directed to the right side, and 23% to the left (positive versus negative PC 1 scores). Hence, about a quarter of the individuals showed the opposite asymmetry pattern than the majority of individuals. The average magnitude of asymmetry along PC 1 was nearly two times larger on the positive side than on the negative side (table S1). In other words, individuals with a reversed pattern of asymmetry showed, on average, a weaker magnitude of asymmetry than the other individuals. Subsequent PCs were more uniformly distributed without a dominance of positive or negative scores (table S1). Because of this absence of directionality, they can be interpreted as different components of fluctuating asymmetry that add to the shared directional asymmetry pattern as captured by PC 1. The first PC accounted for only 19% of total asymmetric variance, with a slow decline in variance for subsequent components (table S1). This suggests that the shared directional asymmetry pattern accounts for only a small part of total asymmetric shape variation. Many more patterns of endocranial asymmetry were present in the sample that together accounted for the remaining 81% of asymmetric variation.

As shown in Fig. 3 and movie S1, this most prevalent or shared pattern of directional asymmetry comprised a differential projection of the occipital lobes: The left lobe had a larger surface area and projected more inferiorly, posteriorly, medially, and laterally than the right one. This was associated with a more inferiolateral projection of the left cerebellar lobe, whereas the right cerebellar lobe bulged

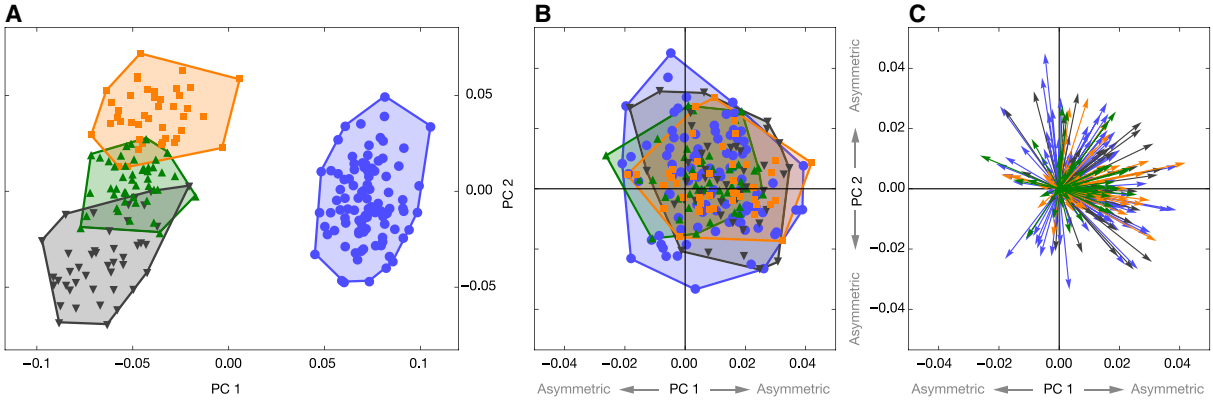

Fig. 2. Symmetric and asymmetric variation of endocranial shape. (**A**) Principal component (PC) analysis of symmetrized endocranial shape. PC 1 versus PC 2 (59.4 and 12.8% of total shape variation, respectively). (**B**) Principal component analysis of endocranial shape asymmetry. PC 1 versus PC 2 (18.8 and 13.8% of total shape asymmetry, respectively). (**C**) Principal component analysis of endocranial shape asymmetry such as in (B), but asymmetry PC scores of each individual are shown as an arrow that represents the individual deviations from symmetry (which corresponds to the origin of the coordinate system). Humans ($n = 95$) are shown in blue, chimpanzees ($n = 47$) in green, gorillas ($n = 43$) in black, and orangutans ($n = 43$) in orange.

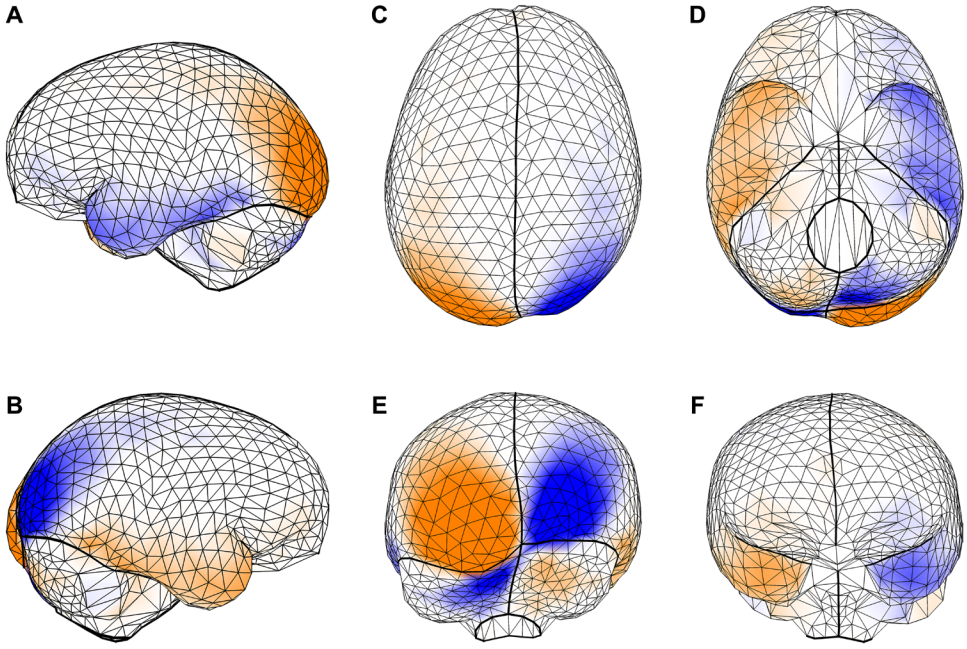

Fig. 3. Shared directional shape asymmetry pattern. PC 1 of endocranial shape asymmetry in Fig. 2B is shown as a triangulated surface mesh of the 935 (semi)landmarks in (**A**) left, (**B**) right, (**C**) superior, (**D**) inferior, (**E**) occipital, and (**F**) frontal views. The deformation from a symmetric endocranial shape represents the spatial pattern of shape asymmetry; orange surfaces have larger areas as compared with the other side, and blue surfaces have smaller areas. See also movie S1.

and protruded more posteriorly ("cerebellar petalia" on the contralateral side of the occipital petalia). Furthermore, the right temporal pole projected more anteromedially and had a larger surface area than the left one. The right frontal lobe projected more anterolaterally and extended more medially as compared with the left lobe. Of all these deviations from symmetry, the occipital lobe contributed most to this combination of local asymmetries or, in other words, to this global spatial pattern of shape asymmetry.

Taxon-specific shape asymmetry

To investigate whether and how directional asymmetry of endocranial shape varies around the shared trend described above, we computed taxon-specific mean asymmetry for humans, chimpanzees, gorillas, and orangutans separately. The spatial patterns of taxon-specific mean asymmetries were reminiscent of the shared pattern found in PC 1 of the pooled PCA (movies S2 to S5). Human mean asymmetry was additionally characterized by a differential projection of the frontoparietal area approximately around the central sulcus, which projected more superiorly on the left side, as well as an asymmetry in the area of the Broca's cap that bulged more and projected more laterosuperiorly on the left side, although its surface area was slightly larger on the right side (movie S2). In chimpanzees, mean asymmetry differed in one aspect from the shared directional asymmetry: It was not the right temporal pole that protruded more anteromedially, but the left one projected slightly more anteroinferiorly, whereas the right one projected slightly more medially (movie S3).

Individual variation in asymmetry

To evaluate the individual expression (or magnitude) of the directional asymmetry pattern, we computed individual shape scores along the mean asymmetry vectors (see Methods). These scores showed that the pattern of directional asymmetry was expressed highly variably across different individuals (length of lines in Fig. 4A). In all four taxa, the distribution of scores was continuous, unimodal, and negatively skewed (skewness of −0.32, −0.14, −0.05, and −0.79 for humans, chimpanzees, gorillas, and orangutans, respectively) and had a mean deviating from zero (i.e., from symmetry). That is, the mean asymmetry pattern in each taxon was highly directional (table S1). In all taxa, however, some individuals showed the opposite of the mean asymmetry pattern (the tail of the distribution with negative scores in Fig. 4A: 17% in humans, 13% in chimpanzees, 9% in gorillas, and 9% in orangutans). But this aspect of endocranial asymmetry was continuously distributed without distinct groups or bimodality (Fig. 4A and see fig. S2 for further explanations).

To elucidate individual variation in the spatial pattern (instead of only the magnitude) of asymmetry, we computed PCAs of shape asymmetry for each taxon separately (Fig. 4C). In these analyses, nonhuman apes had a clearly dominant within-taxon PC 1 (Fig. 4B) that showed a mean clearly distinct from zero (Fig. 4, C and D, and table S1) with the majority of individuals having positive PC 1 scores (83% of chimpanzees, 84% of gorillas, and 81% of orangutans had positive PC 1 scores) and a negative skew (−0.36, −0.28, and −0.27 for chimpanzees, gorillas, and orangutans, respectively). The spatial patterns of asymmetry corresponding to these PC 1s were basically indistinguishable from the taxon-specific mean asymmetry patterns (movies S3 to S5). Within-taxon PC 2 (Fig. 4, C and E) and subsequent PCs of nonhuman apes represented other spatial patterns of asymmetry that did not display clear directionality (table S1; for taxon-specific PC 2s, see movies S3 to S5).

In contrast to the dominant and highly directional first PC in nonhuman apes, humans had two dominant PCs with similar variance (PC 1 and PC 2 accounted for 19 and 18% of total shape asymmetry, while higher PCs had considerably less variance; Fig. 4B). Unlike in nonhuman apes, the pattern of PC 1 was less directed (65% versus 35%; skewness, −0.09) than that of PC 2 (75% versus 25%; skewness, −0.32; Fig. 4, C to E, and table S1), but together, the

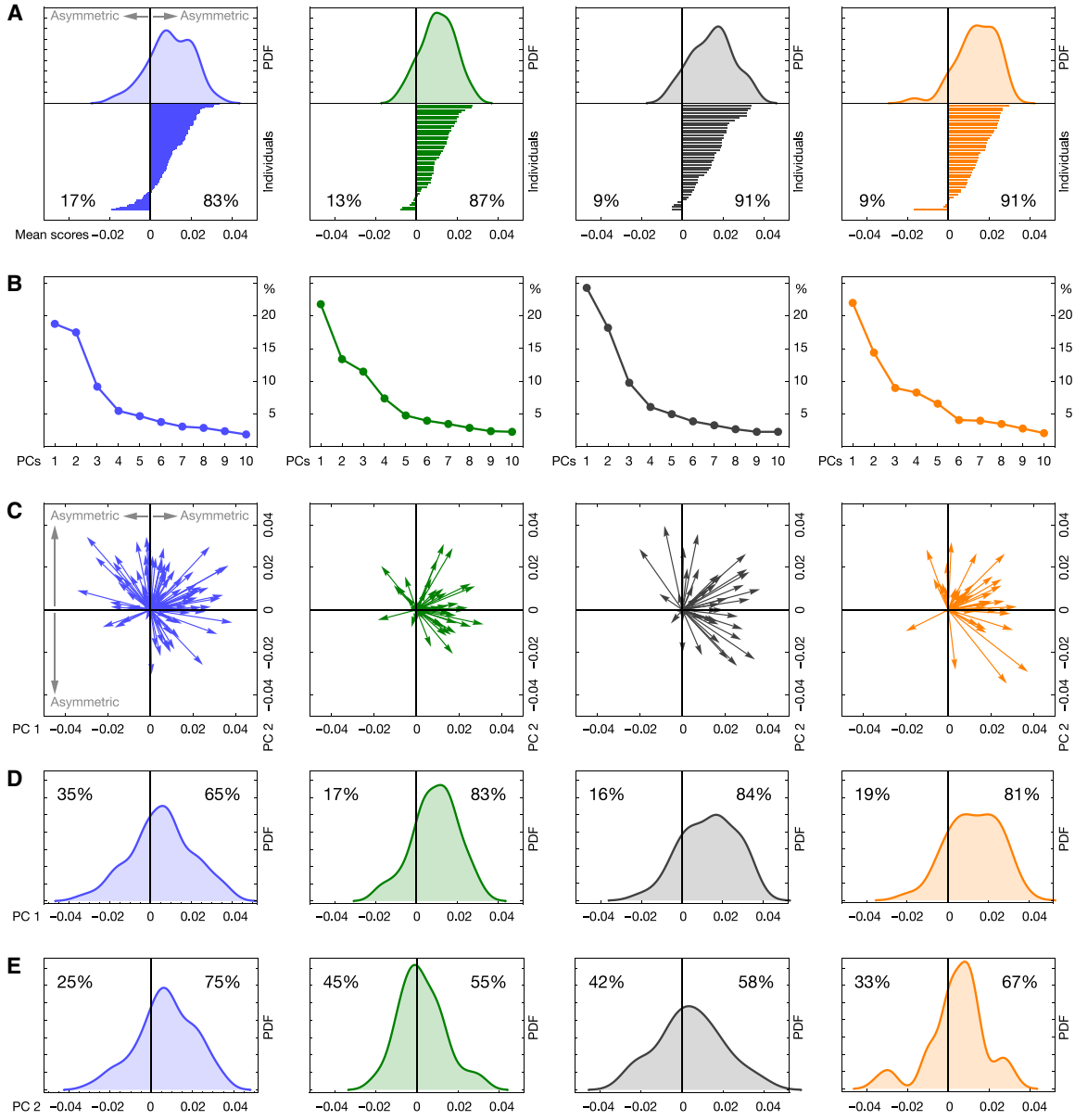

Fig. 4. Asymmetric shape variation within taxa. (**A**) Taxon-specific mean asymmetry. The distribution of individual scores along this asymmetry pattern is shown on top (PDF, probability density function); the actual individual scores are shown below as lines. (**B**) Scree plots for taxon-specific principal component analyses of shape asymmetry display the portion of variance explained by PCs 1 to 10. (**C**) Taxon-specific principal component (PC) analyses of endocranial shape asymmetry. For each taxon, PC 1 versus PC 2 is shown. PC scores are shown as arrows, representing deviations from symmetry (which corresponds to the origin of the coordinate system). (**D** and **E**) Distribution of individuals along the first two taxon-specific PCs. Humans ($n = 95$) are shown in blue, chimpanzees ($n = 47$) in green, gorillas ($n = 43$) in black, and orangutans ($n = 43$) in orange.

two PCs resembled the shared directional asymmetry pattern (movie S2). The major difference between humans and apes is that in nonhuman apes the full directional asymmetry pattern, including the occipital projection together with the contralateral projection of the cerebellar lobe, was represented in a single PC, indicating that these two features of asymmetry covary tightly in the three nonhuman taxa. In humans, by contrast, the same pattern was represented by the sum of two uncorrelated PCs: PC 1 reflected strong occipital lobe and frontal lobe asymmetry combined with a slight cerebellar petalia on the left side, whereas PC 2 showed the typical contralateral asymmetry of occipital and cerebellar lobes together with frontal lobe and Broca's cap asymmetry (movie S2). These findings indicate a decreased correlation and higher variation of frontal, occipital, and cerebellar asymmetries in humans relative to apes. Especially, the combination of occipital and cerebellar asymmetries seems decoupled in humans, indicating a more modular variation of brain asymmetry in humans as compared to nonhuman apes.

Magnitude of shape asymmetry

Independent of the spatial pattern, we also quantified the total magnitude of endocranial asymmetry (Procrustes distances between each individual and its relabeled reflection; see Methods). All analyzed

taxa overlapped in the variation of magnitudes of shape asymmetry. On average, chimpanzees had the lowest magnitude of endocranial shape asymmetry as compared with humans, gorillas, and orangutans ($P < 0.01$ for the pairwise permutation tests of chimpanzees against the other taxa after Bonferroni correction; comparisons among humans, gorillas, and orangutans were not significant; Fig. 5A), but chimpanzees also had the lowest symmetric shape variance (table S2). The fraction of shape variance accounted for by asymmetry, thus, was similar in all four taxa (about 12%). Further decomposing variance in the magnitude of shape asymmetry into directional and fluctuating components (see Methods; table S3) revealed that humans had the lowest degree of directional asymmetry (6.9% of total sample asymmetry) as compared with chimpanzees (11.7%), gorillas (14.8%), and orangutans (13.5%). The average magnitude of fluctuating asymmetry was smallest in chimpanzees as compared with the others ($P < 0.01$ for the pairwise permutation tests of chimpanzees against the other taxa after Bonferroni correction; comparisons among humans, gorillas, and orangutans were not significant; Fig. 5B).

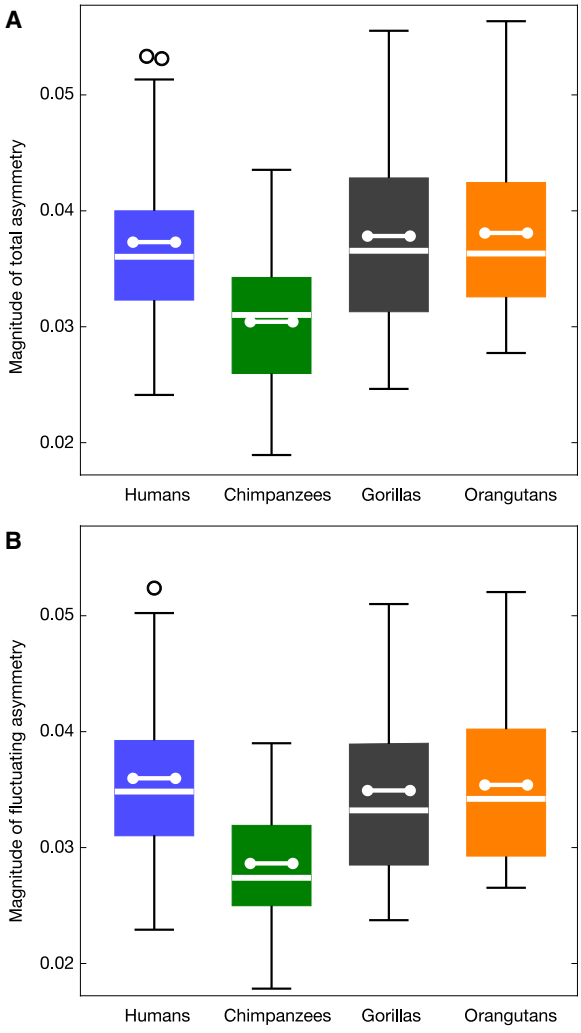

Fig. 5. Magnitude of shape asymmetry. (**A**) Magnitude of total asymmetry (box-whisker plots by taxon). (**B**) Magnitude of fluctuating asymmetry (box-whisker plots by taxon). Humans ($n = 95$) are shown in blue, chimpanzees ($n = 47$) in green, gorillas ($n = 43$) in black, and orangutans ($n = 43$) in orange. Whiskers show the range (outliers as open circles), box and white line show the three quartiles, and the dumbbell represents the average.

Allometric scaling of shape asymmetry

Both within and between taxa, we found only a weak association of endocranial shape asymmetry with endocranial size (fig. S3 and table S4). Between taxa, only 3.3% of shape asymmetry can be explained by size despite the large differences in brain size between humans and nonhuman apes. Within taxa, larger-brained individuals had a slight tendency to show a more pronounced left occipital pole (but only in orangutans this association was close to statistical significance). Otherwise, no consistent association of endocranial asymmetry with size was found.

All the above analyses were based on the asymmetry of endocranial shape. While shape variables do convey information on allometry (the aspects of shape associated with size), absolute size differences had been removed during Procrustes superimposition. To assess absolute asymmetry of endocranial form (shape and size), we re-multiplied the asymmetry vectors with the endocasts' centroid size. The average absolute deviation of all landmarks from symmetry was 1.1 mm in humans and ranged from 0.6 to 0.9 mm in nonhuman apes, reflecting interspecific differences in brain size (human brain volume is three to four times as large as that of nonhuman apes, and thus, linear distances are expected to differ by a factor of $3^{1/3} = 1.4$ to $4^{1/3} = 1.6$). The highest local deviations from symmetry ranged between 5.6 and 5.8 mm in humans, gorillas, and orangutans, and it was 3.6 mm in chimpanzees (table S5). Only 13% of variance in absolute asymmetries can be explained by size in the pooled sample. These relatively small absolute differences reflect the subtle asymmetries of absolute endocranial dimensions and highlight the need for a rigorous quantitative approach for describing petalial patterns.

DISCUSSION

Lateralization of brain functions is widely considered a key characteristic of the human brain that contributes to higher cognitive functions and coincides with anatomical asymmetries of the brain (*2*, *3*, *6*). For instance, a recent study (*5*) concluded that the asymmetry of fronto-occipital petalias is human specific and cannot be found in chimpanzees, but is unrelated to brain size. These authors suggested that a punctual genetic change led to brain lateralization in the hominin lineage. However, although broad comparative studies reported brain asymmetries throughout the animal kingdom (*1*), most studies that emphasized the "uniqueness" of human brain asymmetry relied only on chimpanzee brains for comparison. This neglects the possibility that chimpanzees, not humans, evolved a derived pattern of brain asymmetry. Furthermore, the classic literature presents a somewhat typological view on human brain asymmetry, reporting the proportions of individuals with a specific asymmetric feature and that with the opposite pattern, thus concealing individual variation in the spatial pattern and magnitude of asymmetry. In this study, we focused on anatomical brain asymmetry as reflected by endocast shape, which allowed for a broad comparison across humans, chimpanzees, gorillas, and orangutans, and we used geometric morphometrics and multivariate statistics to quantify individual and taxon-specific variation in magnitude and spatial pattern of endocranial asymmetry. The pervasive individual variation in endocranial asymmetry that we report here, along with asymmetry features shared

across humans and nonhuman apes, demonstrates that the classic typological account of brain asymmetry is too simplistic.

The human pattern of directional asymmetry that we identified, comprising a left occipital and a right frontal petalia, is in accordance with previous findings from human endocasts (*25*, *26*, *28*, *29*) and also from brain imaging studies (*2*, *4*, *5*, *17*). This directional asymmetry pattern was not unique to humans but was shared with chimpanzees, gorillas, and orangutans, partly contradicting previous studies of endocasts (*23*, *25*, *26*, *28*, *29*) and brains (*4*, *5*). While previous work has identified some shared aspects of endocranial asymmetry, for example, the left occipital petalia, our results demonstrate not only that some non-human individuals (*25*, *26*) show the typical human combination of left occipital and right frontal petalias but also that this is the prevalent pattern in all great apes and, therefore, is not unique to humans. This shared spatial hominid pattern of directional asymmetry also comprises a differential projection of the cerebellar lobes and the temporal poles. It is notable, however, that it is least directed in humans as compared with great apes and that the percentage of humans who showed a reversed asymmetry pattern is higher than that of great apes. Our finding of a shared global asymmetry pattern in hominids, along with ample individual variation around this trend, has implications for interpreting endocranial asymmetry in hominin fossils: A left occipital petalia combined with a right frontal petalia found on a fossil hominin endocast does not necessarily indicate a modern human pattern of (functional) brain lateralization because it may simply reflect the shared hominid pattern.

Another unexpected finding was that the individual expression of the global directional asymmetry pattern was not bimodally distributed, as typically expected for antisymmetry (see fig. S2C). In other words, we did not find two distinct groups of individuals, one with the common asymmetry pattern and one with the reversed pattern. Instead, the directional asymmetry pattern was variably expressed in each taxon with a unimodal and slightly negatively skewed distribution that had a mean deviating from zero and a tail with the reversed pattern. As a consequence, those individuals with the reversed asymmetry pattern had, on average, a much weaker magnitude of asymmetry than the individuals with the standard pattern (see fig. S2B). Hence, instead of the typical bimodal distribution of antisymmetry, the reversed endocranial asymmetry pattern is better described as fluctuations around a single directed pattern (fig. S2B). This conclusion is supported by previous studies that also reported unimodal distributions of localized endocranial asymmetric features, such as the anteroposterior component of the occipital petalia (*25*, *26*).

Our results might help to disentangle cause from consequence regarding the emergence of functional and anatomical lateralization of the brain. It seems unlikely that an early functional lateralization causes the directed asymmetric growth of the brain, as this would result in a bimodal distribution of brain and endocranial asymmetry. We hypothesize that functional lateralization is triggered, at least in part, by anatomical brain asymmetry. This could explain the weaker association of functional and anatomical brain lateralization in left-handers than in right-handers, because individuals with a reversed brain asymmetry pattern also have a weaker average magnitude of asymmetry and, thus, a weaker anatomical trigger of functional lateralization.

Yet, the unexpected variable individual expression of the directional asymmetry pattern is only a small part of the full picture. We found that directional asymmetry explains only 7% of asymmetric shape variation in humans and 12 to 15% in great apes, confirming that fluctuating asymmetry, not directional asymmetry, accounts for most of the asymmetric variation in the brain (*17*). The amount of fluctuating asymmetry was similar in humans, gorillas, and orangutans; only chimpanzees had a decreased shape asymmetry, consistent with a recent study based on brain magnetic resonance imaging (MRI) data (*17*). While the latter study interpreted this as the result of an evolutionary increase of brain asymmetry in the human lineage, our results show that chimpanzees have decreased asymmetry relative to humans and other nonhuman apes (but chimpanzees also showed the least symmetric endocranial shape differences). These differences might be affected by the composition of our samples: Chimpanzees are represented mostly by one subspecies of *Pan troglodytes*, while subspecies information for gorillas and orangutans is often not available (see Methods for more details). But the fraction of shape variation that accounted for asymmetry—which is largely independent of sample composition—was very similar in all four taxa (about 12%). Thus, our findings using humans, chimpanzees, gorillas, and orangutans challenge the view that differences between humans and chimpanzees indicate higher developmental plasticity in humans (*17*). On the other hand, sulcual variation that was not captured by our landmark set was shown to be less heritable in humans than in chimpanzees and may, thus, have a higher degree of plasticity in humans (*38*).

Humans differed from the other apes in another characteristic of their endocranial asymmetry. Whereas in nonhuman apes, the directional asymmetry pattern was the most dominant one, accounting for most of asymmetric variation (as depicted by the taxon-specific PC 1s; Fig. 4B), humans had two dominant asymmetry patterns with similar variance (human-specific PC 1 and PC 2, accounting for 19 and 18% of total variance, respectively; Fig. 4B). The more directed pattern was the one with slightly less variance (PC 2; Fig. 4E) and corresponded to the directional pattern shared with great apes (PC 1; Figs. 2B and 3). The other pattern was only weakly directed (PC 1; Fig. 4D) and resembled the shared directional pattern in the frontal and occipital petalias but was differently associated with cerebellar asymmetry (movie S2). This indicates that—even though humans and nonhuman apes show a similar average pattern of asymmetry—the asymmetry of the different endocranial regions is less integrated in humans than in great apes.

A recent study (*6*) found that functional lateralization is distributed along four partly independent axes: symbolic communication, perception/action, emotion, and decision making. This "modular" functional lateralization in humans might be reflected by our finding of a more decoupled or dissociated anatomical brain asymmetry compared with nonhuman apes (*39*). Different cerebellar regions were shown to be dominantly activated in the symbolic communication axis (posterior cerebellar lobe) and the perception/action axis (anterior cerebellum and part of the vermis); however, in both cases, the right side was dominant (*6*).

Our finding that cerebellar and occipital asymmetry are decoupled in humans is interesting in the context of cerebellar evolution in the human lineage. Nonhuman apes and also our closest extinct relatives, the Neanderthals, do not have a large and rounded cerebellum (*40*). The expansion of the cerebellum during early brain development evolved only recently in *Homo sapiens* (*41*), and the analysis of introgressed Neanderthal genes into modern humans revealed that brain globularity, including a bulging cerebellum, is related to the expression of two genes, one of which regulates myelination in the cerebellum (*42*). The decoupling of cerebellar and occipital asymmetry reported here may be related to this recent evolutionary expansion

of the cerebellum and reflect evolutionary changes in neural connectivity between the cerebellum and the cerebrum.

It has been previously suggested that functionally lateralized brain regions show less connectivity through the corpus callosum to the other hemisphere than nonlateralized regions, and therefore, it was argued that lateralization can avoid conduction delays between the hemispheres of the larger human brain (*6*). Our study, however, showed that the total magnitude of endocranial shape asymmetry cannot be explained by size, confirming the findings of a previous MRI study of human and chimpanzee brains (*17*). Furthermore, the spatial pattern of asymmetry that was weakly associated with increasing brain size only partly resembled the shared directional asymmetry pattern. The lack of a clear association between endocranial size and fluctuating shape asymmetry in our data is also at odds with the expectation that larger brains, which grew longer and/or faster than small brains, accumulated more developmental instabilities and, thus, show increased fluctuating asymmetry.

Some limitations of our study are important to discuss. While endocranial asymmetry, as captured by our landmark set, closely reflects asymmetry of global brain shape, asymmetries of brain convolutions (sulci and gyri) are not well represented by our data. However, while not directly comparable to brain data, using endocranial data, we were able to broaden the comparative scope of our analysis beyond mere human-chimpanzee comparisons. Our analyses would require to be replicated with brain MRI data. Future studies should also investigate interrelationships of the magnitude and spatial pattern of asymmetry in the brain, the endocranium, the cranial base, and the face. A possible confounder is measurement error, which often is asymmetric. Random error largely cancels in estimates of directional asymmetry but is an inherent component of fluctuating asymmetry. Our analysis of repeated measurements in 20 individuals (see Methods and fig. S4) demonstrated that measurement error (Procrustes distance between repeated measurements) was of similar magnitude in all four taxa and, thus, is unlikely to account for the interspecific asymmetry differences reported here. Measurement error was less than the smallest individual shape differences and even less than the smallest shape asymmetry in our sample. Asymmetry scores and PC scores were reliably replicated (fig. S4). Although measurement error inevitably inflates estimates of fluctuating asymmetry, our findings on individual variation and average patterns of endocranial asymmetry are very unlikely to result from measurement error.

In conclusion, humans and nonhuman apes share a conserved directional pattern of endocranial shape asymmetry and are similar in the overall magnitude of shape asymmetry. Only chimpanzees showed a reduced magnitude of both symmetric and asymmetric shape variation, which questions interpretations of human "uniqueness" inferred from a comparison with chimpanzees only. Our results also emphasize the need to disentangle shape asymmetry from absolute size differences, which might have concealed the shared asymmetry pattern among hominids in earlier studies. Instead of a unique spatial asymmetry pattern with strong directionality, humans display a uniquely variable and decoupled pattern of local asymmetries with reduced directionality relative to nonhuman apes. The dissociation of the shared hominid asymmetry pattern in humans (especially the decoupling of occipital and cerebellar petalias) may be a key factor in creating the wide individual asymmetric variation in humans and likely reflects increased functional and developmental modularization of the human brain.

METHODS

Sample

Our sample comprised dried adult crania of 95 humans, 47 chimpanzees, 43 gorillas, and 43 orangutans. The human sample included individuals from Africa, Asia, Europe, and the Americas, covering a wide range of cranial variation. Common chimpanzees encompassed 33 *P. troglodytes verus*, 1 *P. troglodytes troglodytes*, 1 *P. troglodytes schweinfurthii*, and 12 individuals of unknown subspecies. Gorillas were mostly *Gorilla gorilla* except for two *Gorilla beringei graueri* individuals. Orangutans were mostly *Pongo pygmaeus* but included also one *Pongo abelli* and three individuals of unknown species. Our sample of great apes included predominantly individuals that have been living in their natural habitat (for eight chimpanzees, one gorilla, and two orangutans, this information was not available).

Human individuals were from the anatomical collections of the University of Leipzig and the University of Vienna. Nonhuman apes were from the American Museum of Natural History, the Naturhistorisches Museum Wien, the Museum für Naturkunde Berlin, the Smithsonian National Museum of Natural History, the Max Planck Institute for Evolutionary Anthropology, and the University College London.

Computed tomography data and digital endocasts

All data were captured on digital representations derived from computed tomography (CT) scans of the dried crania. This enabled noninvasive access to the endocranium without destroying or harming the original specimens.

Human individuals from the University of Leipzig and chimpanzee individuals from the Taï National Forest (Côte d'Ivoire) housed at the Max Planck Institute for Evolutionary Anthropology had been CT scanned with a BIR ACTIS 225/300 industrial CT scanner at the Max Planck Institute for Evolutionary Anthropology. Gorillas and orangutans from the Museum für Naturkunde Berlin had been scanned with a Philips Ingenuity Core 128 CT scanner at the Vivantes Klinikum Berlin. Humans from the University of Vienna and chimpanzees from the Naturhistorisches Museum Wien had been scanned with a Siemens Sensation 16 and Siemens Plus 4 Volume Zoom CT scanner. CT scans of other human and ape individuals have been acquired from digital databases including the Open Research Scan Archive of the University of Pennsylvania, Museum of Archaeology and Anthropology (www.penn.museum/sites/orsa/Welcome.html), the 3D collection of the Smithsonian National Museum of Natural History (http://humanorigins.si.edu/evidence/3d-collection/primate), and NESPOS (www.nespos.org/). The CT data from the various sources had a pixel size ranging from 0.18 to 0.5 mm and a slice thickness ranging from 0.18 to 1 mm (most of the scans had a pixel size of about 0.3 mm and a slice thickness of about 0.5 mm). Asymmetry measures did not show any correlation with image resolution, indicating that our results are not affected by differences in CT scan resolution. For all individuals, we generated digital endocasts from the CT scans by a combination of semiautomated segmentation in Avizo (Thermo Fisher Scientific), including threshold functions and manual adjustments as detailed in (*36*).

Landmark data

We quantified endocranial shape by a geometric morphometric approach (*30*, *31*) based on 935 endocranial landmarks (*36*, *43*), including sliding semilandmarks on several curves and the endocranial surface (fig. S1) (*32*). We used curve semilandmarks to compartmentalize

the endocranial surface. The cerebellar surface, for example, was delimited from the cerebral surface by a curve along the superior border of the transverse sinus. For more details on the landmark set, see (*36*, *41*).

For quantifying asymmetry, every landmark and semilandmark on the left side had a corresponding (homologous) landmark or semilandmark on the right side ("paired landmarks"; see Fig. 1D). In addition to these 892 paired points (446 on the left side and 446 on the right side), the landmark set also contained 43 unpaired landmarks and semilandmarks, which can show a signal of asymmetry whenever they deviate from the global midsagittal plane. To remove asymmetry resulting from an asymmetric placing of semilandmarks along curves and surfaces (as opposed to actual anatomical asymmetry), semilandmarks were allowed to slide to a symmetrized template configuration (*34*). Since semilandmarks slid on tangents to the curves and surface until their bending energy (a measure of local shape difference) to the symmetric template shape was a minimum, we projected them back to the corresponding curve or surface and iterated these steps until convergence (*32*). This procedure resulted in geometric point-to-point correspondences of the semilandmarks within the sample and removed both symmetric and asymmetric shape differences that resulted from the initial location of semilandmarks rather than genuine morphological differences, including endocranial asymmetry.

The local anatomical midplane between the foramen cecum on the rostral end of the endocast and the attachment site of the tentorium cerebelli at the caudal end was represented by a curve. Both the sagittal suture and the superior sagittal sinus, connected to the falx cerebri in between the two hemispheres, are not always observable on endocasts and can be highly variable and asymmetric themselves. Hence, to cope with this ambiguity, we measured a best-fit global midsagittal plane, but the semilandmarks of this midsagittal "curve" were not treated as curve semilandmarks but were allowed to slide on the endocranial surface. In other words, the demarcation between the left and right hemispheres at the cranial vault is not explicitly represented in our data because it cannot be exactly inferred from the endocast alone; instead the semilandmarks of the midsagittal curve trace the overall left-right asymmetry of the cerebral hemispheres.

Disentangling symmetric shape and shape asymmetry

We reflected and relabeled the landmark configuration of each individual (*30*, *34*) (ensuring that the left landmarks were compared with the reflected right landmarks, and the right landmarks were compared with the reflected left ones). All configurations and their reflections were superimposed together by a generalized Procrustes analysis (*30*). This removed the variation in location, orientation, and scale from the raw coordinates, resulting in Procrustes shape variables along with centroid size as a measure of overall size. We averaged each landmark configuration and its superimposed relabeled reflection, resulting in symmetric shapes. The sample of these "symmetrized" configurations served as the basis for studying symmetric shape variation. It gave rise to a symmetric shape space, in which—for our data—each configuration is represented by a 935 × three-dimensional data point (with 2798 degrees of freedom). Furthermore, we computed the difference between each landmark configuration and its superimposed relabeled reflection (a 935 × three-dimensional vector with 1378 degrees of freedom) representing the specimen's shape asymmetry (*30*, *31*). Because the symmetric and asymmetric shape spaces are orthogonal, the fractions of symmetric and asymmetric shape variation could be inferred from the total sample variances in the two spaces (*34*). It is important to note that this Procrustes approach did not require the specification of an anatomical midplane to compute asymmetry because the superimposition of the landmark configuration and its reflection are based on all landmarks, not only the midsagittal (unpaired) landmarks, which tend to be asymmetric themselves.

Analysis of endocranial shape variation

We computed a standard PCA of the symmetrized Procrustes shape variables.

Analysis of the pattern and magnitude of shape asymmetry

To explore the multivariate patterns of asymmetry, we performed a slightly modified version of PCA. In contrast to the original Procrustes coordinates, the asymmetry vectors have a meaningful origin: Zero indicates symmetry. We, thus, computed PCs of the asymmetry vectors that maximize the sum of squares around the symmetric origin, not around the asymmetric sample mean (as in standard PCA). This allowed for a least-squares ordination of the asymmetry vectors as multivariate deviations from symmetry that can be interpreted in terms of pattern and magnitude (instead of deviations from their sample mean, which would correspond to the fluctuating asymmetry component only). Computationally, this was achieved by singular value decomposition (SVD) of the raw data matrix of asymmetry vectors (whereas standard PCA results from an SVD of the mean-centered data matrix). As the first singular vector of a data matrix is close to the sample mean vector (as long as it deviates from zero), the first principal component tends to align with the pattern of directional asymmetry (average of asymmetry vector). Histograms of the corresponding PC scores allowed for the assessment of directionality and antisymmetry. This analysis was performed for the pooled sample to investigate shared aspects of endocranial asymmetry and also separately for each taxon to address taxon-specific patterns.

To further study directional asymmetry, we computed the mean of the asymmetry vectors for each taxon. We computed directional asymmetry scores by projecting each individual onto its normalized taxon-specific mean asymmetry vector and analyzed histograms of these scores to assess directionality and antisymmetry.

The spatial patterns of shape asymmetry were visualized using a triangulated mesh of the landmark set as endocranial surface. To highlight left-right differences between local surface areas, we used color coding as explained in (*43*). Regions with surface areas deviating 97 to 103% from symmetry were shown in white. Regions with larger surface areas were shown in orange (>115%), regions with smaller surface areas were shown in blue (<85%). Values in between were shown as different shades of orange or blue. Note that this color coding is different from color maps typical in brain imaging that represent the magnitude but not the direction of local deformation (corresponding to a single scalar per landmark). Our visualizations illustrate both magnitude and pattern of shape asymmetry (a 3D vector per landmark) as seen from the deformed surface (the deviation from a symmetric endocranial shape).

Independent of the spatial pattern, we quantified the total magnitude of endocranial shape asymmetry by the Procrustes distances between each individual and its relabeled reflection (which is twice the magnitude of the deviation from symmetry). We computed the magnitude of fluctuating asymmetry by the Procrustes distance between each individual, and its relabeled reflection after taxon-specific directional asymmetry had been removed. We compared

within-taxon variation in the magnitude of total and fluctuating asymmetry using box-whisker plots. Furthermore, we determined the fractions of the directional and fluctuating components in a sum-of-squares decomposition of total asymmetry (*33*, *34*).

Asymmetry and allometry

We computed regressions of the magnitude of total asymmetry on the logarithm of centroid size and determined the percentage of variance explained by size. Furthermore, we computed shape regressions on the logarithm of centroid size, correlated shape regression scores with the logarithm of centroid size, and visualized the spatial pattern of endocranial asymmetry related to increasing endocranial size in each taxon.

Measurement error and repeatability

Measurement error inflates estimates of fluctuating asymmetry because it is a measure of variance, not mean. For some traits, measurement error can even be similar in magnitude to measures of asymmetry (*11*, *33*, *34*). However, random measurement error does not contribute considerably to estimates of directional asymmetry because it is a mean. To evaluate the degree to which measurement error influences our measures of shape asymmetry, we measured 19 individuals twice (7 humans and 4 of each nonhuman taxon). Note that measurement error here did not only include inconsistences of landmark placing (intra- and interobserver error) but also how these landmarks were affecting the sliding process of semilandmarks.

In absolute terms, the difference between the two measurement sessions was 0.6 mm on average per (semi)landmark, and 95% of all (semi)landmarks measured for these 19 individuals differed less than 1.8 mm. Procrustes distances between repeated measurements of the 19 individuals were smaller than the smallest Procrustes distance between different individuals of a given taxon, demonstrating that measurement error generally did not affect our ability to distinguish between two different individuals of the same taxon (fig. S4A). Procrustes distances between repeated measurements were similar in humans, chimpanzees, gorillas, and orangutans (fig. S4A); i.e., measurement error was comparable in magnitude among all four measured taxa. Measurement error, thus, was unlikely to be the reason for our finding that chimpanzees were less asymmetric in magnitude than the other taxa. Furthermore, Procrustes distances between repeated measurements were even smaller than the smallest Procrustes distance between any individual and its relabeled reflection, demonstrating that measurement error was smaller than measurements of asymmetry. Magnitudes of asymmetry were very similarly estimated in the repeated-measurements sessions (fig. S4B).

In addition, we measured another human individual five times and superimposed these values on the figures showing the main results (fig. S4, C to F). Again, while measurement error was visible, the repeated measures led to very similar directional asymmetry scores, PC scores, and magnitudes of asymmetry, suggesting that measurement error did not considerably affect the asymmetry signal reported here. In absolute terms, the mean deviation from symmetry in these five repeated measurements of one individual was consistently between 1.2 and 1.3 mm and thus also representative of the average human absolute asymmetry.

Effects of sample size and composition

While our chimpanzee sample included only one species (*P. troglodytes*), the *G. gorilla* and *P. pygmaeus* samples included a few individuals from another species (see above). Furthermore, our human sample was larger than each of the ape samples. To investigate potential effects of sample composition and size on our results, we performed additional analyses based on the largest possible subsamples of equal size that represented single species: a random subsample of 39 individuals out of 95 humans, a random subsample of 39 *P. troglodytes* out of 47 chimpanzees, a random subsample of 39 *G. gorilla* out of 43 gorillas, and the subsample of 39 *P. pygmaeus* out of 43 orangutans. These analyses (fig. S5) closely replicated the reported results. Differences in sample composition, thus, are very unlikely to affect our conclusions.

SUPPLEMENTARY MATERIALS

Supplementary material for this article is available at http://advances.sciencemag.org/cgi/content/full/6/7/eaax9935/DC1

Fig. S1. Endocranial landmark set.
Fig. S2. Classic types of asymmetry and shape asymmetry.
Fig. S3. Relationship of shape asymmetry and endocranial size.
Fig. S4. Measurement error in repeated measurements analyses.
Fig. S5. Effects of sample size and composition.
Table S1. Descriptive statistics of PCA.
Table S2. Symmetric and asymmetric variance in units of squared Procrustes distance per taxon.
Table S3. Magnitudes of sample asymmetries decomposed into directional and fluctuating components.
Table S4. Variance of shape asymmetry explained by log centroid size, with *P* values (permutation test) for the variance explained.
Table S5. Descriptive statistics of absolute deviations from symmetry.
Movie S1. Shared directional shape asymmetry.
Movie S2. Human-specific asymmetry patterns.
Movie S3. Chimpanzee-specific asymmetry patterns.
Movie S4. Gorilla-specific asymmetry patterns.
Movie S5. Orangutan-specific asymmetry patterns.

REFERENCES AND NOTES

1. M. C. Corballis, I. S. Häberling, The many sides of hemispheric asymmetry: A selective review and outlook. *J. Int. Neuropsychol. Soc.* **23**, 710–718 (2017).
2. A. W. Toga, P. M. Thompson, Mapping brain asymmetry. *Nat. Rev. Neurosci.* **4**, 37–48 (2003).
3. X.-Z. Kong, S. R. Mathias, T. Guadalupe; ENIGMA Laterality Working Group, D. C. Glahn, B. Franke, F. Crivello, N. Tzourio-Mazoyer, S. E. Fisher, P. M. Thompson, C. Francks, Mapping cortical brain asymmetry in 17,141 healthy individuals worldwide via the ENIGMA Consortium. *Proc. Natl. Acad. Sci. U.S.A.* **115**, E5154–E5163 (2018).
4. L. Xiang, T. J. Crow, W. D. Hopkins, Q. Gong, N. Roberts, Human torque is not present in chimpanzee brain. *Neuroimage* **165**, 285–293 (2018).
5. L. Xiang, T. Crow, N. Roberts, Cerebral torque is human specific and unrelated to brain size. *Brain Struct. Funct.* **224**, 1141–1150 (2019).
6. V. R. Karolis, M. Corbetta, M. Thiebaut de Schotten, The architecture of functional lateralisation and its relationship to callosal connectivity in the human brain. *Nat. Commun.* **10**, 1417 (2019).
7. M. D. Cykowski, O. Colulon, P. V. Kochunov, K. Amunts, J. L. Lancaster, A. R. Laird, D. C. Glahn, P. T. Fox, The central sulcus: An observer-independent characterization of sulcal landmarks and depth asymmetry. *Cereb. Cortex* **18**, 1999–2009 (2008).
8. J.-F. Mangin, D. Riviere, A. Cachia, E. Duchesnay, Y. Cointepas, D. Papadopoulos-Orfanos, D. L. Collins, A. C. Evans, J. Regis, Object-based morphometry of the cerebral cortex. *IEEE Trans. Med. Imaging* **23**, 968–982 (2004).
9. L. E. White, G. Lucas, A. Richards, D. Purves, Cerebral asymmetry and handedness. *Nature* **368**, 197–198 (1994).
10. Z. Y. Sun, S. Klöppel, D. Rivière, M. Perrot, R. Frackowiak, H. Siebner, J.-F. Mangin, The effect of handedness on the shape of the central sulcus. *Neuroimage* **60**, 332–339 (2012).
11. A. R. Palmer, C. Strobeck, Fluctuating asymmetry: Measurement, analysis, patterns. *Annu. Rev. Ecol. Syst.* **17**, 391–421 (1986).
12. M. Annett, *Left, Right, Hand and Brain: The Right Shift Theory* (Lawrence Erlbaum Associates, London, 1985).
13. A. Gomez-Robles, W. D. Hopkins, S. J. Schapiro, C. C. Sherwood, The heritability of chimpanzee and human brain asymmetry. *Proc. R. Soc. B Biol. Sci.* **283**, 20161319 (2016).

14. A. N. Gilbert, C. J. Wysocki, Hand preference and age in the United-States. *Neuropsychologia* **30**, 601–608 (1992).
15. W. D. Hopkins, in *Cerebral Lateralization and Cognition: Evolutionary and Developmental Investigations of Behavioral Biases*, G. S. Forrester, W. D. Hopkins, K. Hudry, A. Lindell, Eds. (Academic Press, 2018), pp. 57–89.
16. S. V. Dongen, Fluctuating asymmetry and developmental instability in evolutionary biology: Past, present and future. *J. Evol. Biol.* **19**, 1727–1743 (2006).
17. A. Gomez-Robles, W. D. Hopkins, C. C. Sherwood, Increased morphological asymmetry, evolvability and plasticity in human brain evolution. *Proc. R. Soc. B Biol. Sci.* **280**, 20130575 (2013).
18. M. C. Corballis, What's left in language? Beyond the classical model. *Ann. N. Y. Acad. Sci.* **1359**, 14–29 (2015).
19. D. Stout, T. Chaminade, Stone tools, language and the brain in human evolution. *Philos. Trans. R. Soc. B Biol. Sci.* **367**, 75–87 (2012).
20. P. M. Greenfield, Language, tools, and brain: The ontogeny and phylogeny of hierarchically organized sequential behavior. *Behav. Brain Sci.* **14**, 531–551 (1991).
21. C. L. R. Gonzalez, N. A. van Rootselaar, R. L. Gibb, Sensorimotor lateralization scaffolds cognitive specialization. *Prog. Brain Res.* **238**, 405–433 (2018).
22. M. L. Moss, R. W. Young, A functional approach to craniology. *Am. J. Phys. Anthropol.* **18**, 281–292 (1960).
23. R. L. Holloway, D. C. Broadfield, M. S. Yuan, *The Human Fossil Record: Brain Endocasts—The Paleoneurological Evidence* (John Wiley & Sons, Inc., 2004).
24. S. Neubauer, Endocasts: Possibilities and limitations for the interpretation of human brain evolution. *Brain Behav. Evol.* **84**, 117–134 (2014).
25. A. Balzeau, E. Gilissen, Endocranial shape asymmetries in *Pan paniscus*, *Pan troglodytes* and *Gorilla gorilla* assessed via skull based landmark analysis. *J. Hum. Evol.* **59**, 54–69 (2010).
26. A. Balzeau, E. Gilissen, D. Grimaud-Hervé, Shared pattern of endocranial shape asymmetries among great apes, anatomically modern humans, and fossil hominins. *PLOS ONE* **7**, e29581 (2012).
27. A. Balzeau, E. Gilissen, R. L. Holloway, S. Prima, D. Grimaud-Herve, Variations in size, shape and asymmetries of the third frontal convolution in hominids: Paleoneurological implications for hominin evolution and the origin of language. *J. Hum. Evol.* **76**, 116–128 (2014).
28. R. L. Holloway, M. C. De La Costelareymondie, Brain endocast asymmetry in pongids and hominids - some preliminary findings on the paleontology of cerebral-dominance. *Am. J. Phys. Anthropol.* **58**, 101–110 (1982).
29. M. Lemay, Morphological cerebral asymmetries of modern man, fossil man, and nonhuman primate. *Ann. N.Y. Acad. Sci.* **280**, 349–366 (1976).
30. F. L. Bookstein, *Morphometric Tools for Landmark Data Geometry and Biology* (Cambridge Univ. Press, Cambridge, 1991), pp. XVII+435P.
31. P. Mitteroecker, P. Gunz, Advances in geometric morphometrics. *Evol. Biol.* **36**, 235–247 (2009).
32. P. Gunz, P. Mitteroecker, F. L. Bookstein, in *Modern Morphometrics in Physical Anthropology*, D. E. Slice, Ed. (Springer US, 2005), pp. 73–98.
33. C. P. Klingenberg, G. S. McIntyre, Geometric morphometrics of developmental instability: Analyzing patterns of fluctuating asymmetry with procrustes methods. *Evolution* **52**, 1363–1375 (1998).
34. K. V. Mardia, F. L. Bookstein, I. J. Moreton, Statistical assessment of bilateral symmetry of shapes. *Biometrika* **87**, 285–300 (2000).
35. T. Bienvenu, F. Guy, W. Coudyzer, E. Gilissen, G. Roualdes, P. Vignaud, M. Brunet, Assessing endocranial variations in great apes and humans using 3D data from virtual endocasts. *Am. J. Phys. Anthropol.* **145**, 231–246 (2011).
36. S. Neubauer, P. Gunz, J.-J. Hublin, Endocranial shape changes during growth in chimpanzees and humans: A morphometric analysis of unique and shared aspects. *J. Hum. Evol.* **59**, 555–566 (2010).
37. N. Scott, S. Neubauer, J.-J. Hublin, P. Gunz, A shared pattern of postnatal endocranial development in extant hominoids. *Evol. Biol.* **41**, 572–594 (2014).
38. A. Gómez-Robles, W. D. Hopkins, S. J. Schapiro, C. C. Sherwood, Relaxed genetic control of cortical organization in human brains compared with chimpanzees. *Proc. Natl. Acad. Sci. U.S.A.* **112**, 14799–14804 (2015).
39. P. Mitteroecker, The developmental basis of variational modularity: Insights from quantitative genetics, morphometrics, and developmental biology. *Evol. Biol.* **36**, 377–385 (2009).
40. T. Kochiyama, N. Ogihara, H. C. Tanabe, O. Kondo, H. Amano, K. Hasegawa, H. Suzuki, M. S. P. de León, C. P. E. Zollikofer, M. Bastir, C. Stringer, N. Sadato, T. Akazawa, Reconstructing the Neanderthal brain using computational anatomy. *Sci. Rep.* **8**, 6296 (2018).
41. S. Neubauer, J.-J. Hublin, P. Gunz, The evolution of modern human brain shape. *Sci. Adv.* **4**, eaao5961 (2018).
42. P. Gunz, A. K. Tilot, K. Wittfeld, A. Teumer, C. Y. Shapland, T. G. M. van Erp, M. Dannemann, B. Vernot, S. Neubauer, T. Guadalupe, G. Fernandez, H. G. Brunner, W. Enard, J. Fallon, N. Hosten, U. Volker, A. Profico, F. Di Vincenzo, G. Manzi, J. Kelso, B. St Pourcain, J. J. Hublin, B. Franke, S. Pääbo, F. Macciardi, H. J. Grabe, S. E. Fisher, Neandertal introgression sheds light on modern human endocranial globularity. *Curr. Biol.* **29**, 120–127.e5 (2019).
43. S. Neubauer, P. Gunz, in *Digital Endocasts: From Skulls to Brains*, E. Bruner, N. Ogihara, H. C. Tanabe, Eds. (Springer-Verlag Tokyo, Tokyo, 2018), pp. 173–190.

Acknowledgments: We are grateful for the critical and constructive comments by A. Gomez-Robles and A. Balzeau during the review process. We thank all curators, technicians, and institutions who made the acquisition and usage of CT scans possible, including C. Boesch, C. Feja, K. Helgen, B. Herzig, N. Lange, F. Mayer, P. Schönefeld, P. Schubert, U. Olbrich-Schwartz, K. Spanel-Borowski, F. Spoor, H. Temming, M. Tocheri, G. W. Weber, A. Winzer, the University of Leipzig, the University of Vienna, University College London, Naturhistorisches Museum Wien, Naturkundemuseum Berlin, American Museum of Natural History New York, Smithsonian's Division of Mammals and Human Origins Program, Smithsonian 2.0 Fund, Smithsonian's Collections Care and Preservation Fund, Ivorian Ministries of the Environment and Forests and of Research, Swiss Center for Scientific Research Abidjan, Open Research Scan Archive of the University of Pennsylvania, 3D collection of the Smithsonian National Museum of Natural History, and NESPOS. **Funding:** This work was supported by the Max Planck Society and the Austrian Science Fund (FWF P29397). **Author contributions:** S.N., P.G., and P.M. designed the research. S.N. and N.A.S. collected the data. S.N. analyzed the data. S.N., P.G., P.M., and J.-J.H. interpreted the data. S.N., P.G., and P.M. wrote the paper. **Competing interests:** The authors declare that they have no competing interests. **Data and materials availability:** All data needed to evaluate the conclusions in the paper are present in the paper and/or the Supplementary Materials. All landmark data analyzed in this paper may be requested from the authors.

Submitted 10 May 2019
Accepted 22 November 2019
Published 14 February 2020
10.1126/sciadv.aax9935

Citation: S. Neubauer, P. Gunz, N. A. Scott, J.-J. Hublin, P. Mitteroecker, Evolution of brain lateralization: A shared hominid pattern of endocranial asymmetry is much more variable in humans than in great apes. *Sci. Adv.* **6**, eaax9935 (2020).